Field stress path simulation of rain-induced slope failure

Simulation du chemin de contraintes d'une rupture de talus causée par la pluie

R. P. BRENNER, Senior Geotechnical Engineer, Electrowatt Engineering Services Ltd., Zürich, Switzerland
H. K. TAM, Geotechnical Engineer, Moh and Associates (S) Pte. Ltd., Singapore
E. W. BRAND, Principal Government Geotechnical Engineer, Engineering Development Department, Hong Kong

SYNOPSIS Special procedures of laboratory triaxial tests were developed to simulate the field stress path of an element of soil along a potential failure surface in a fill slope subjected to rainwater infiltration. Such an element will usually be in an unsaturated state with a negative pore pressure (suction) acting. When rainwater enters the slope, the pore pressure will increase while the total stress essentially remains constant. Modelling of this process was accomplished by conducting dead load tests on compacted specimens of a volcanic residual soil with specified initial conditions. Five dead load tests on back-saturated specimens and ten tests on unsaturated specimens, preconditioned to a specified suction, were carried out. In all but one test, failure was generated by increasing the pore pressure; in the remaining test the specimen was sheared by decreasing the cell pressure. The data obtained from these tests, although limited, permit some insight into the relationship between the mode of failure (i.e. dilatant or compressive) and the placement conditions of a fill. They should be useful for the design of fill slopes for which compressive volumetric strain behaviour during rain infiltration should be avoided.

INTRODUCTION

Planning and construction activities for urban development in hilly terrain covered by residual soils will frequently confront the geotechnical engineer with stability problems. This applies to both, cut and fill slopes, as well as to potentially unstable natural slopes. The upper part of a residual soil profile is invariably unsaturated, but usually has a relatively high permeability to infiltrating rainwater. The controlling factor governing the stability of slopes in such soils is the distribution of the pore water pressure, both with positive and with negative sign, along the potential failure surface. The relative ease by which rainwater is able to enter residual soil profiles obviously causes the pore water pressure regime to be governed largely by the pattern of rainfall. Good correlations between rainfall intensity and frequency of landslides have been reported in the literature for various geographical locations, e.g. Hong Kong (Lumb, 1975), Japan (Fukuoka, 1980), New Zealand (Crozier, 1969), and the United States (Nilsen et al, 1976).

When rainwater infiltrates a soil profile which is in an unsaturated state, a decrease in pore suction (negative pore pressure) occurs. This causes a decrease in the effective normal stress acting along the potential failure plane, which in turn diminishes the available shear strength. Disregarding the negligible increase in bulk unit weight of the soil by the infiltrating rainwater, the process leading to failure of the soil essentially takes place under constant total stress conditions, i.e. σ_1 and σ_3 remain constant while the pore pressure is increasing (Brand, 1981, 1982).

Thus the stress path followed by a soil element on a potential failure plane in a slope subjected to rain infiltration is obviously different from that in a conventional triaxial compression test in which σ_3 remains constant and σ_1 is increasing. The difference in stress path implies further that the stress ranges over which triaxial tests are usually conducted are not appropriate to the field conditions. In order to obtain meaningful shear properties from laboratory tests for analysis and design of slopes, it is necessary to simulate the field stress path as closely as possible. The only way to model the rain-induced failure mechanism correctly, is by conducting constant (dead) load tests in which the pore pressure increases from an initially negative value until failure is observed. Rodin et al (1982) conducted dead load tests on specimens which were first wetted up by percolation. A pore water pressure increase was then achieved by means of a hand pump introducing water.

In this paper the results of two kinds of dead load test are reported, namely (i) dead load tests on saturated specimens and (ii) on unsaturated specimens. In both cases failure was generated by increasing the pore water pressure at constant total stress, but only the latter type truly simulated field behaviour. The data so obtained are analyzed with reference to the failure mode and are applied to the design of fill slopes subjected to severe rain infiltration.

EXPERIMENTAL PROCEDURE

Materials tested

The soil used in this study was taken from a borrow area in Tai Po, Hong Kong. This material is a colluvium derived from a residual volcanic soil. For laboratory testing, the soil was processed through a 20 mm BS (British Standard) sieve. The relevant physical and chemical properties of the material are summarized in Table I. All classification tests were conducted in accordance with the procedures given in BS 1377:1975 and were performed on air-dried soil.

TABLE I

Material Properties

Property	Unit	Typical range
Sand (2.0-0.06 mm)	% by weight	18 ± 1
Silt (0.06-0.002 mm)	% by weight	47 ± 2
Clay (< 0.002 mm)	% by weight	35 ± 2
Specific gravity	-	2.71 ± 0.02
Liquid limit	%	58 ± 2
Plastic limit	%	29 ± 2
Linear shrinkage	%	11
Organic matter	%	0.28 ± 0.03
pH value	-	4.5 ± 0.3
Colour	-	light yellow to yellowish red

Testing program and specimen preparation

In this paper the results of five series of dead load tests are reported. These tests were part of a comprehensive testing program to evaluate the stress-strain and strength characteristics of residual, unsaturated soils with respect to slope stability problems. The initial conditions of each series are summarized in Table II. The series DLS refers to back-saturated and the series DLU to unsaturated compacted specimens.

The moisture - dry density relationship of the material was established from twelve standard Proctor tests performed according to BS 1377:1975, Test 12. The maximum dry density (MDD) and the optimum moisture content (OMC) were 1.55 Mg/m^3 and 24.5% respectively. From these values the initial conditions given in Table II were obtained.

The test specimens were then prepared by statically compacting, in three layers, known weights of material into a mold of known dimensions. Typical specimen dimensions after extrusion from the mold were 49.6 mm in diameter and 99 mm in height.

TABLE II

Testing Program and Initial Conditions of Specimens

Series no.	Number of specimens	Isotropic consolidation pressure (kPa)	Deviator stress (kPa)	Specified initial conditions %MDD	e_o	w (%)
DLS-1-30	1	100	160	85	1.03	24.5
	2*	200				
	1	400				
DLS-2-30	1	200	160	95	0.84	24.5
DLU-1	4	0	73	85	1.03	24.5
		10	101			
		30	160			
		60	204			
DLU-2	3	0	73	90	0.94	24.5
		10	101			
		30	160			
DLU-3	3	0	73	95	0.84	24.5
		10	101			
		30	160			

Note: MDD = Maximum dry density (BS)
e_o = Initial void ratio
* DLS-1-30-200A: by increasing pore water pressure
DLS-1-30-200B: by decreasing cell pressure

Selection of stress range

In order to model realistically the stress range applicable to shallow slope failures in the dead load tests, an estimate was made by employing the resistance envelope concept (Janbu, 1977). For a slope with a given geometry and strength parameters, the average shear stress, τ_{av}, and the average normal stress, σ'_{av}, calculated along an arbitrary slip surface can be plotted as a point in a (τ_{av}, σ'_{av})-diagram. The resistance envelope for the slope considered is then an upper boundary curve enveloping all such points obtained from a number of trial surfaces. A typical fill slope of similar material as used for the test series was selected to establish the resistance envelope in terms of total stresses in the $(\sigma_1+\sigma_3)/2$ vs. $(\sigma_1-\sigma_3)/2$ plane. From this plot and by comparison with the stress conditions in an infinite slope, the range of anisotropic consolidation stresses given in Table II for the DLU series could be derived.

Testing procedures

DLS test series The test specimens were set up between a top and a bottom low-air-entry porous stone and fitted with two 0.3 mm thick rubber membranes. Before saturation, a cell pressure of 30 kPa was applied to prevent swelling of the specimen during saturation. Then the cell pressure was applied through both the bottom and the top drainage line. To achieve full saturation a back pressure of 600 kPa with a duration of five to six days was required. Volume changes of cell water and pore water pressures were monitored throughout the entire testing phase.

Isotropic consolidation was performed in stages to the levels specified in Table II. The next stage was applied when 95% pore pressure dissipation had been achieved from the previous stage. Upon completion of isotropic consolidation, dead loads in increments of 44.5 N were applied to the ram by means of a light-weight hanger. The rate of load application was governed by the 95% dissipation of pore pressure criterion.

For bringing the specimen to failure two techniques were tried, viz.: (i) by increasing the pore water pressure and (ii) by decreasing the cell water pressure. Both procedures yield the same stress path, but only the first one models the failure mechanism correctly.

In the first procedure, the back pressure applied through the top drainage line was increased in increments of 20 kPa. Upon equalization of pore pressure, which was ascertained by taking readings also at the bottom drainage line, the volume change in cell water, the amount of water which entered the specimen, the axial strain, and the final value of pore water pressure were recorded. The diameter of the specimen was measured with a travelling telescope mounted on a vernier gauge. Failure was indicated when after an increment of back pressure steady deformation of the specimen could be observed.

In the second procedure (used with test DLS-1-30-200B), the cell pressure was decreased in decrements of 20 kPa. The pore water pressure at the top of the specimen was held constant and the amount of pore water inflow at the base, as well as the axial deformation, were measured after pore pressure equalization. Failure was reached when the specimen could no longer sustain the dead load as indicated by a steady increase in the axial strain. All test results of the DLS series were corrected for effects of rubber membrane stiffness.

DLU test series All specimens were initially at optimum water content, but each series was carried out at a different %MDD. The specimen was set up between a saturated high-air-entry (3 bar) ceramic disc at its bottom and a dry low-air-entry porous stone at the top. The base of the ceramic disc was connected to a transducer and then to a mercury pot system for controlled suction, as shown in Fig. 1. The top cap was vented to atmosphere. (It may be assumed that for shallow slip surfaces the pore air pressure remains atmospheric during rain infiltration and only the pore water pressure is increased).

It was necessary to first precondition the compacted unsaturated specimens, as they had in general a suction greater than 100 kPa, in order to prevent cavitation of the water in the measuring system. By appropriate positioning of the pots in the mercury pot system, a specific pore water tension would be produced which could be measured by the transducer. This tension could then be applied to the ceramic disc and water would flow into the specimen (which was at a higher suction). The magnitude of controlled suction was then decreased in steps until the specified initial value of 80 kPa for running the test was achieved. Each step required 6 to 24 hours for pore water pressure equalization, and five days were needed to complete preconditioning.

After preconditioning, the specimen was first isotropically and then anisotropically consolidated to the total stress conditions given in Table II. Dead loads for anisotropic consolidation were applied in increments of 44.5 N and the axial deformation recorded. After complete anisotropic consolidation shearing was initiated by the following steps: Valve V1 was closed and valve V2 opened (Fig. 1). The mercury pot system was adjusted such that a suction of 10 kPa lower than that in the specimen could be applied. Burette B1 was read for the initial water level and then valve V1 opened again. This caused water to enter the specimen with a subsequent decrease in suction which in turn caused the specimen to deform. The amount of water inflow was read from burette B1 and the change in negative pore pressure with time observed. Upon equalization of pore pressure, changes in volume of cell water, axial strain and final value of pore water pressure were recorded. This procedure was repeated in steps of 10 kPa decrements of suction until the specimen failed. The air drainage line remained open throughout the test in order to maintain atmospheric pressure. Equilibration of pore pressure after each decrement required 6 to 24 hours; hence each test needed 10 to 14 days to complete. It was necessary to correct the observed volume change of cell water for the water displaced by the movement of the ram into the cell.

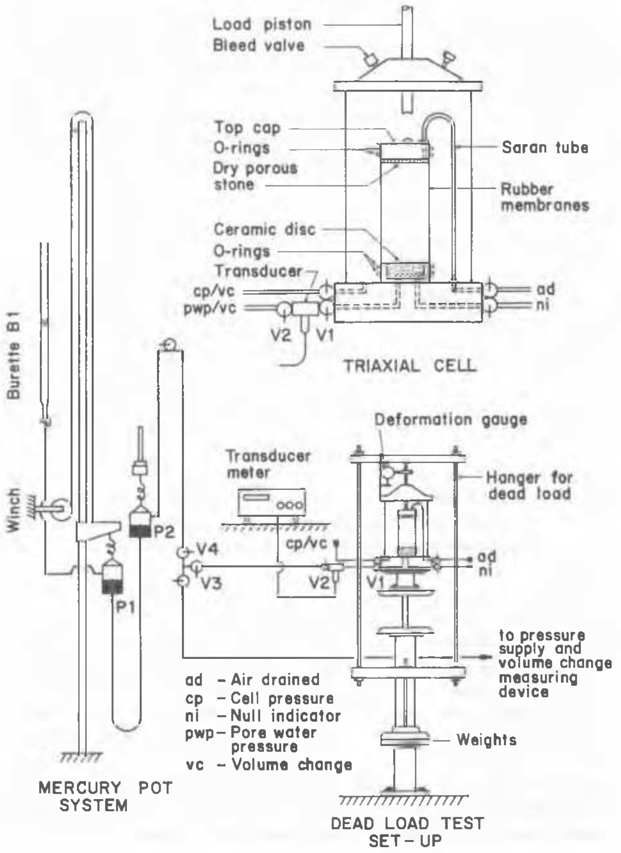

Fig. 1 Set-up for DLU test series

TEST RESULTS AND DISCUSSION

Dead load tests on back-saturated specimens (DLS tests)

Figure 2 shows the variation of pore water pressure, major and minor principal effective stress, obliquity, volumetric strain, and specific volume with axial strain. Of interest is the comparison of test DLS-1-30-200B, in which failure was generated by decreasing the cell pressure, with the other four tests. It can be seen from Fig. 2a that for this test the pore pressure slowly decreased (see also Fig. 3b). Figure 2b illustrates how both the major and minor principal stresses decrease as the specimen is sheared. For test DLS-1-30-200B the total vertical stress had to be adjusted with the decrease in cell pressure in order to maintain the deviator stress at a constant level. The obliquity for all tests of the DLS-1-30 series sheared by an increasing pore pressure is about the same (Fig. 2c). It appears that for a given density the strength is independent of the pre-shear consolidation pressure. The volumetric strain (Fig. 2d) at a given axial strain increases with increasing pre-shear consolidation pressure for specimens with the same initial density (series DLS-1-30). If, on the other hand, the specific volume is considered (Fig. 2e), almost identical curves are obtained.

Figure 3 shows a comparison of the variation of specific volume, υ, with pore water pressure for tests DLS-1-30-200A and DLS-1-30-200B. A similar picture is obtained when instead of υ the water content is plotted. In Fig. 3a, a tangent line has been drawn to both ends of the curve. The point of intersection may be interpreted as the condition at which the specimen starts yielding without further significant increase in pore water pressure.

Finally, Fig. 4 shows the effective stress paths for all five DLS tests. Also shown are failure envelopes obtained from three series of isotropically consolidated, drained, strain-controlled triaxial compression tests, denoted by CDS-1, CDS-2, and CDS-3, representing conventional testing practice. The back-saturated specimens of these three series had initial %MDD of 95, 100, and 105 respectively. It can be seen that for maximum obliquity (Fig. 2c) the corresponding points of the DLS-1-30 specimens coincide more or less with the failure envelope of the CDS-2 test

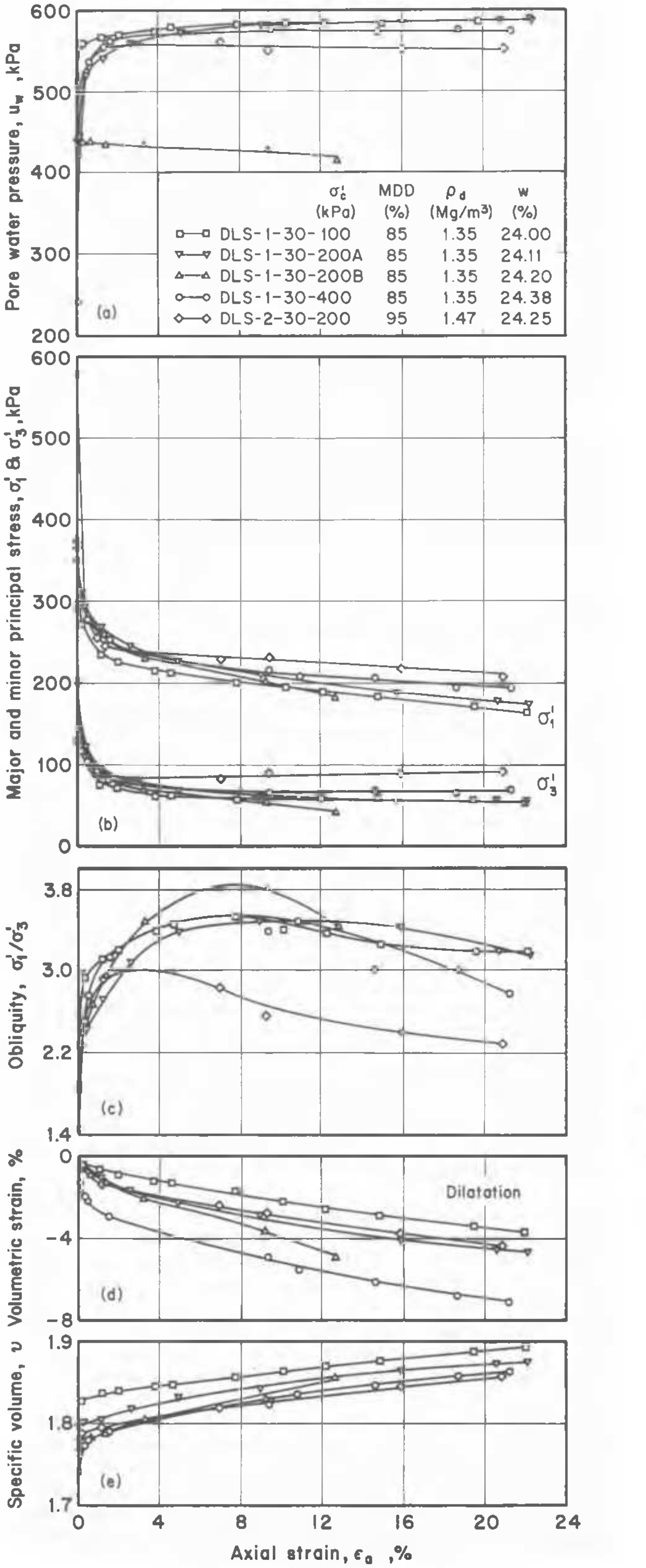

Fig. 2 Variation of pore pressure, major and minor principal stress, obliquity, volumetric strain, and specific volume with axial strain (DLS test series)

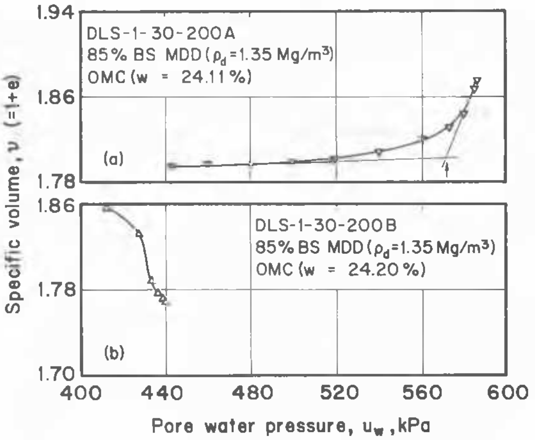

Fig. 3 Variation of specific volume with pore water pressure: (a) for test DLS-1-30-200A sheared by increasing the pore water pressure, and (b) for test DLS-1-30-200B sheared by decreasing the cell pressure

series. Those specimens of the CDS-2 series which were isotropically consolidated at 100 and 200 kPa pressure had almost identical densities and water contents before shearing as the specimens DLS-1-30-100 and DLS-1-30-200 after anisotropic consolidation, although the initial densities after compaction were 100 and 85% MDD respectively. Saturation of dense compacted specimens may lead to swelling, and subsequent consolidation under low confining stresses may not give the previously specified density at which the test should be conducted. Hence the strength measured in the test is underestimated. On the other hand, it is speculated that a low density specimen may collapse during saturation and densify, leading to a higher strength than that which would be available in situ. A factor of safety based on such data would then be overestimated.

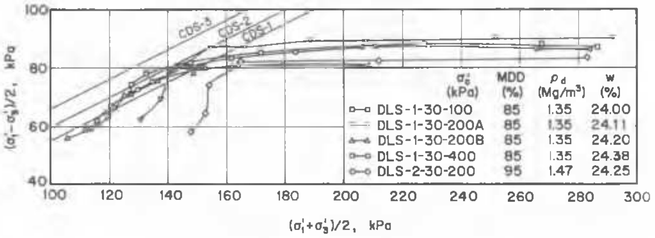

Fig. 4 Effective stress paths of specimens of DLS test series and comparison with failure envelopes from conventional (drained) triaxial compression tests

Dead load tests on unsaturated specimens (DLU tests)

Selected results of the DLU tests are given in Figs. 5 to 7. Figure 5a presents the suction ($-u_w$) vs. axial strain relationship for series DLU-1. It may be seen that for tests DLU-1-0 and DLU-1-10 the suction reached a limiting value of about 43 kPa. For these specimens the failure mode was dilatant (Fig. 6a). Dilatation of a specimen induces additional suction which counteracts losses in suction caused by infiltrating water. For tests DLU-1-30, on the other hand, the suction continued to drop with increasing strain, because the failure mode was compressive. With this mode of failure the decrease in volume will further

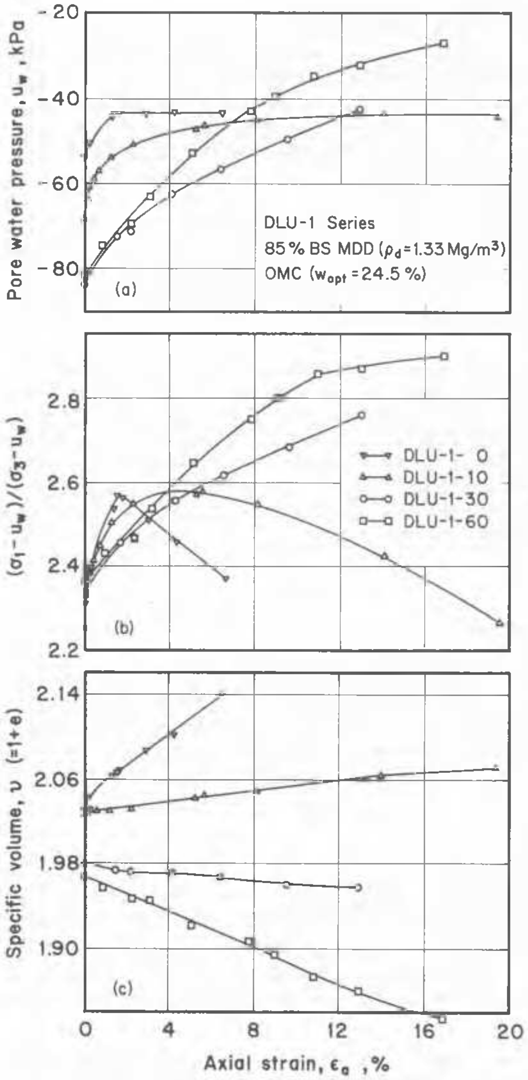

Fig. 5 Variation of pore water pressure (suction), principal stress ratio, and specific volume with axial strain for DLU-1 series

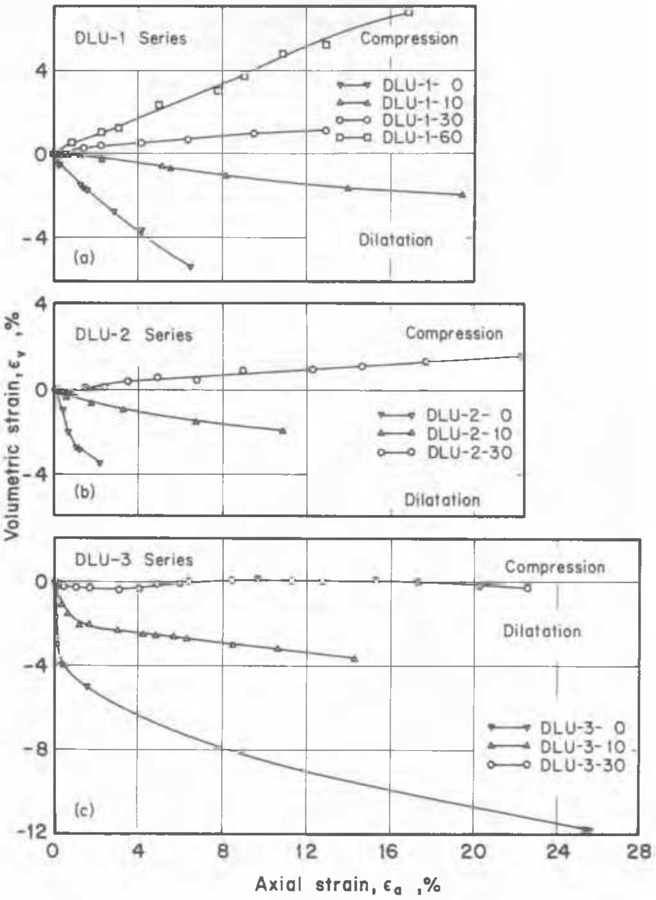

Fig. 6 Variation of volumetric strain with axial strain for DLU-1, DLU-2, and DLU-3 series.

reduce the amount of suction, thus accelerating deformation. In Fig. 5b, the principal stress ratio of the DLU-1 series has been plotted. It can be noted that the strength of the specimens with a dilatant failure mode decreases rapidly after a pronounced peak has been exceeded. The variation of specific volume with axial strain is shown in Fig. 5c and indicates the compressive and dilatant behaviour of the specimens of series DLU-1.

Figure 6 illustrates the variation of volumetric strain with axial strain for all three DLU series. It can be seen that with higher initial densities and for a given pre-shear consolidation stress the failure mode tends to become dilatant.

Finally, Fig. 7 shows the variation of specific volume, water content, and degree of saturation with suction for the DLU-1 series. The specific volume of specimens with consolidation pressures of 0 and 10 kPa increased with decrease in suction, but for specimens with higher consolidation pressures (i.e. 30 and 60 kPa) it decreased with a reduction in suction (Fig. 7a). The water content of all specimens increased with decreasing suction (Fig. 7b). The degree of saturation increased with decreasing suction for all specimens except for those which were unconfined (Fig. 7c). With the unconfined specimens the saturation initially increased or remained stationary with decreasing suction, but at a certain critical value of suction it dropped abruptly because the specimen started to dilate appreciably. Similar results as shown in Figs. 5 and 7 were also observed with series DLU-2 and DLU-3.

Application to fill slope design

It was observed that specimens of the DLU series with low initial density when wetted up under constant total stress fail in a dilatant mode when the pre-shear consolidation stress is low (i.e. 0 and 10 kPa in the case of the DLU-1 series); otherwise the specimens fail in a compressive mode. From these observations it follows that there must be a critical consolidation pressure, p_c, for which no volume change occurs when a soil element is wetted up under constant total stress. Through interpolation from Fig. 6, it is possible to estimate p_c for the initial conditions given in Table II. Assuming now an infinite slope, a critical thickness or depth, z_c, of fill associated with p_c may be computed. Values of p_c and z_c, calculated for the resistance envelope selected for this study,are given in Table III.

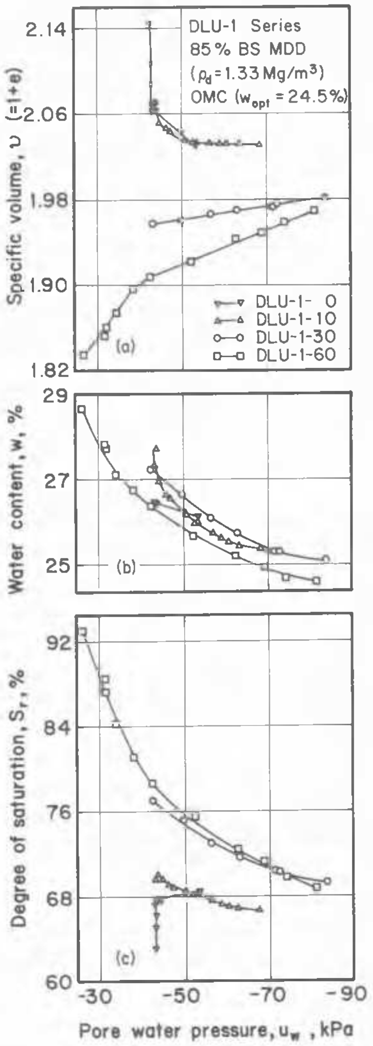

Fig. 7 Variation of specific volume, water content and degree of saturation with pore water pressure (suction) for DLU-1 series

TABLE III

Critical Pressure and Equivalent Depth of Fill for Different Placement Conditions

Series	Specified placement conditions			p_c	z_c
	% BS MDD	Dry density ρ_d (Mg/m³)	w (%)	(kPa)	(m)
DLU-1	85	1.33	24.5	20	4.3
DLU-2	90	1.40	24.5	25	4.9
DLU-3	95	1.47	24.5	30	5.5

For the design of a fill slope with a given geometry, resistance envelope and fill height, the placement conditions should be specified such that the critical fill thickness, z_c, is not exceeded.

CONCLUSIONS

The tests and their results presented here are a new approach to simulate experimentally the mechanism of rain-induced slope failure. The tests are delicate and time-consuming to run. Based on the data available from this study, the principal observations may be formulated as follows:

(1) Limited test results indicate that conventional triaxial compression tests may yield different strength parameters than obtained with DLS tests which simulate the field stress path, and they may thus lead to an incorrect assessment of the stability of a slope.

(2) The failure mode (i.e. dilatant or compressive) of unsaturated specimens wetted up under constant total stress depends on the initial density and the pre-shear consolidation pressure. There exists a critical pressure at which there is no volume change. This observation should be useful in the design of fill slopes for which a compressive volumetric strain behaviour during rain infiltration should be avoided.

ACKNOWLEDGMENT

The tests reported herein were conducted at the Material Testing Laboratory, Public Works Department, Hong Kong. The authors gratefully acknowledge the cooperation given by Messrs. M.D. Howat, J.M. Shen, K.L. Lai and C.H. Hui.

REFERENCES

Brand, E.W. (1981). Some thoughts on rain-induced slope failures. Proc. 10th ICSMFE, 3, 373-376, Stockholm.

Brand, E.W. (1982). Analysis and design in residual soils. Proc. ASCE Specialty Conf. Engineering and Construction in Tropical and Residual Soils, 89-143, Honolulu.

Crozier, M.J. (1969). Earthflow occurrence during high intensity rainfall in Eastern Otago. Engineering Geology (3), 325-334.

Fukuoka, M. (1980). Landslides associated with rainfall. Geotechnical Engineering (11), 1-29.

Janbu, N. (1977). Slopes and excavations in normally and lightly overconsolidated clays. In: Slopes and Excavations, N.R. Morgenstern et al, Proc. 9th ICSMFE, 2, 549-566, Tokyo.

Lumb, P. (1975). Slope failures in Hong Kong. Quarterly J. Engineering Geology (8), 31-65.

Nilsen, T., Taylor, F.A. and Brabb, E.E. (1976). Recent landslides in Alameda County, California (1940-71): An estimate of economic losses and correlations with slope, rainfall, and ancient landslide deposits. U.S. Geological Survey, Bulletin 1398, 24p. + 1 drg.

Rodin, S., Henkel, D.J. and Brown, R.L. (1982). Geotechnical study of a large hillside area in Hong Kong. Hong Kong Engineer (10), 5, 37-45.